Aptamer based electrochemical sensor for detection of human lung adenocarcinoma A549 cells

Aptamer based electrochemical sensor for detection of human lung adenocarcinoma A549 cells

Rachna Sharma[1, 3], Ved Varun Agrawal[1], Pradeep Sharma[2], R Varshney[2], R K Sinha[3] and B D Malhotra[4]

[1]Biomedical Instrumentation Section, National Physical Laboratory, Dr. K.S. Krishnan Marg, New Delhi 110012, India

[2]Institute of Nuclear Medicine & Allied Sciences, Lucknow Road, Timarpur, Delhi 110 054, India

[3]Department of Applied Physics, Delhi Technological University, Main Bawana Road, Delhi 110042, India

[4]Department of Biotechnology, Delhi Technological University, Main Bawana Road, Delhi 110042, India

E-mail: bansi.malhotra@gmail.com   or   bansi.malhotra@dce.ac.in

Abstract. We report results of the studies relating to development of an aptamer-based electrochemical biosensor for detection of human lung adenocarcinoma A549 cells. The aminated 85-mer DNA aptamer probe specific for the A549 cells has been covalently immobilized onto silane self assembled monolayer (SAM) onto ITO surface using glutaraldehyde as the crosslinker. The results of cyclic voltammetry and differential pulse voltammetry studies reveal that the aptamer functionalized bioelectrode can specifically detect lung cancer cells in the concentration range of 10^3 to 10^7 cells/ml with detection limit of 10^3 cells/ml within 60 s. The specificity studies of the bioelectrode have been carried out with control KB cells. No significant change in response is observed for control KB cells as compared to that of the A549 target cells.

1. Introduction

Lung cancer is currently a major cause of cancer related deaths both in the developed and developing nations[1-3]. To reduce high mortality rate arising due to lung cancer, an early diagnosis of the disease is essential. Most of the existing methods presently being used for cancer detection are X-ray, spiral computed tomography[4], sputum cytology[5], positron emission tomography[6], virtual bronchoscopy[7] etc .These methods are based on morphological criteria that cannot be used for early detection of this important disease. Besides this, these are known to be non-specific for cancer classification. Since cancer results from the accumulation of a variety of genetic events (e.g., mutations, rearrangements, and deletions)[8-12] controlling cell growth and differentiation, the studies on these changes may perhaps serve as diagnostically useful molecular markers[13-15]. Development of molecular probes that

---

[4]   To whom any correspondence should be addressed.

can recognize molecular abnormalities during the lung carcinogenesis process is likely to enable clinicians for diagnosis of cancer at early stage and identify its subtypes.

Development of noninvasive tests has been the focus of cancer research that may facilitate earlier diagnosis and treatment of lung cancer. Several studies on variation of the surface specific antigens to differentiate between normal and cancer cells have been performed using antibodies[16]. These surface [1] specific antigens cannot be exclusively expressed for any single type of cells and may result in false-positivity. To address to this problem, aptamers have emerged as attractive alternatives to antibodies[17,18]. Aptamers, single-stranded oligonucleotides, have been identified for specific cancer cell recognition by applying a cell-SELEX (cell-based systematic evolution of ligands by exponential enrichment) method[19]. Besides this, these biomolecules can fold into unique three dimensional conformations to bind to selected molecules ranging in size from small organic molecules to whole cells with high affinity and selectivity[20].

Aptamers are known to possess several advantages over other recognition molecules like ease of synthesis and modification, long term stability, high specificity etc which making these biomolecules as potential candidates for development of desired analytical devices[21]. Several studies relating to the fabrication of aptamer based biosensors for the detection of proteins[22], molecules[23], cancer cells[24-27] etc have been performed indicating high affinity and specificity of the aptamer probes towards their respective targets. And the electrochemical method of detection is being preferred over other methods of detection since this technique exhibits high signal to noise ratio resulting in high sensitivity, rapid response and reproducibility of the biosensor[28]. Pan et al have fabricated an aptamer based electrochemical sensor for label-free recognition and detection of leukemia cells[26]. Rodriguez et al have reported an aptamer based biosensor for lysozyme detection using electrochemical impedance spectroscopy[29].

In the present manuscript, we report results of studies relating to fabrication of an electrochemical biosensor for detection of lung cancer cells using aptamers. The aptamer functionalized bioelectrode has been prepared by covalent immobilization of the aptamer probe on self assembled monolayer of silane onto the ITO surface using glutaraldehyde as the crosslinker. The response of the bioelectrode towards the target cancer cells has been investigated using cyclic voltammetry and differential pulse voltammetry.

2. Materials and methods

3-(2-aminoethylamino) propyl trimethoxysilane (AEAPTS), glutaraldehyde and amine-terminated aptamer sequence have been purchased from Sigma-Aldrich. All the reagents are of analytical grade and have been used without further purification. De-ionized water (Milli Q 10 TS) with resistivity >18.2 MΩ-cm has been used for preparing all aqueous solutions. Indium-tin-oxide (ITO) coated glass plates have been obtained from Balzers, UK, (Baltracom 247 ITO, 1.1 mm thick) with sheet resistance and transmittance 25 Ωsq^{-1} and 90%, respectively.

Aptamer probe: NH$_2$ - 5'- ACG CTC GGA TGC CAC TAC AGG GTT GCA TGC CGT GGG GAG GGG GGT GGG TTT TAT AGC GTA CTC AGC TC ATG GAC GTG CTG GTG AC -3'[30]

Target cells: A549 cells

Control cells: KB cells

2.1. Culture medium for cells

A549 cells derived from human lung adenocarcinoma and KB (control) cells derived from head and neck squamous carcinoma are maintained as monolayer cultures at 37 °C in a humidified CO$_2$ incubator (5% CO$_2$, 95% air). A549 and KB cells are maintained in high glucose DMEM supplemented with 10% fetal bovine serum (FBS), HEPES (10 mM) and antibiotics (30 μgml^{-1} penicillin G, 50 μgml^{-1} streptomycin and 2 μgml^{-1} nystatin). All the cell lines are routinely sub-cultured (twice a week) using 0.05 % trypsin in 0.02 % EDTA and reseeded in fresh medium. FBS and DMEM (both low and high glucose) were purchased from SIGMA chemicals.

2.2. Fabrication of Aptamer-functionalized bioelectrode
ITO coated glass plates are washed with acetone, ethanol and copious amount of deionized water followed by hydrolyzation in $NH_4OH:H_2O_2:H_2O$ (1:1:5) solution at 80°C for 45 min. Hydrolyzed ITO plates are dipped in 1% ethanolic solution of AEAPTS for 2 h for formation of self-assembled monolayer (SAM) and then washed with ethanol followed by deionized water. Silanized ITO surfaces are then soaked in 0.5% aqueous solution of glutaraldehyde for 6 h for SAM formation. Glutaraldehyde acts as a crosslinker between the amine group at the silanized ITO surface and the amine-terminated aptamer sequence. 20 µL of 1 µM aptamer solution is then dispensed onto the silanized ITO surface for about 2 h for covalent immobilization resulting in the fabrication of aptamer functionalized bioelectrode.

2.3. Characterization
The morphology of the aptamer functionalized bioelectrode and morphological changes on incubation of the bioelectrode with target cells have been studied using SEM, LEO 440 scanning electron microscope. The transmission studies of the silanized ITO surface and the aptamer functionalized bioelectrode in the infrared region have been carried out on Perkin Elmer, Spectrum BX II spectrophotometer in the wavenumber range of 4000-450 cm^{-1}.

The electrochemical experiments have been conducted on Autolab PGSTAT 302N System (Ecochemie, The Netherlands) in a three electrode system. All electrochemical experiments have been carried out in a cell containing 15 ml of 100 mM Phosphate Buffer Solution (PBS, pH 7.4) containing 0.9% NaCl and 5 mM $K_3/K_4[Fe(CN)_6]$ as a redox probe and using a platinum wire as auxiliary, a Ag/AgCl wire as reference, and the modified ITO as the working electrode.

3. Results and discussion

3.1. SEM studies
Figure 1 shows the morphology obtained for the apt-glu-silane-ITO bioelectrode before and after cell binding. The observed granular structure on immobilization of single-stranded DNA aptamer indicates covalent binding of aminated aptamer probe onto silanized ITO surface (figure 1(a)). The uniform spindle like structure appears on incubation of the apt-glu-silane-ITO bioelectrode with A549 cells (figure 1(b)) revealing the affinity of aptamers with target cells.
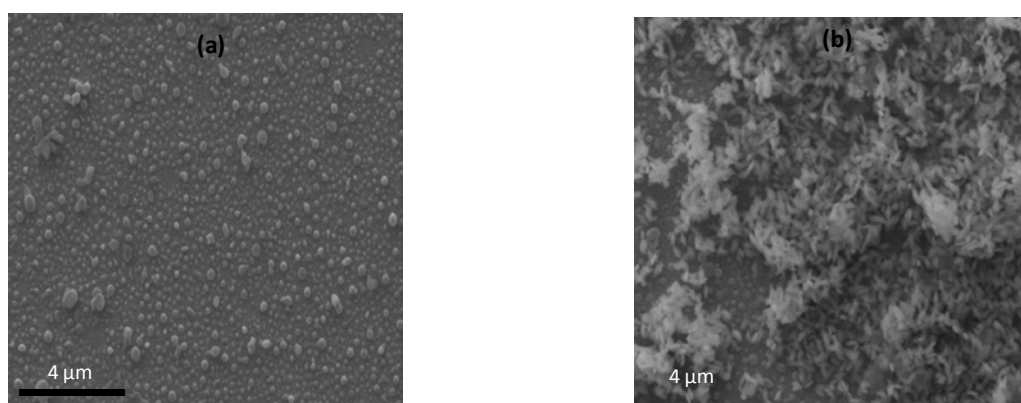

Figure 1. SEM micrographs of apt-glu-silane-ITO bioelectrode before (a) and after (b) cell binding.

3.2. FTIR studies
Figure 2 shows the transmittance spectra observed for the silanized ITO electrode and aptamer functionalized bioelectrode. The peaks seen at 679 cm^{-1} and 1113 cm^{-1} corresponding to Si-CH$_3$ stretch and Si-O-Si antisymmetric stretch respectively, indicate the formation of siloxane bond between the

silane and the ITO surface[31] [figure 2(a)]. Peaks found at 1415 cm^{-1}, 2808 cm^{-1} and 3265 cm^{-1} correspond to C-N, C-H and N-H stretch in the AEAPTS, respectively. Further, the peak at 1585 cm^{-1} corresponding to NH$_2$ deformation reveals the presence of amine groups at the silanized ITO surface.
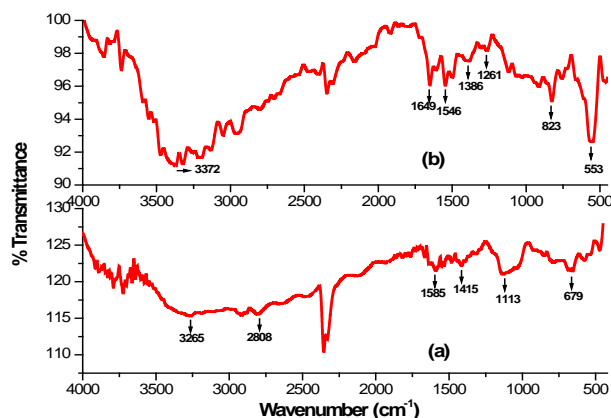

Figure 2. FTIR spectra of (a) AEAPTS/ITO surface and; (b) Apt/Glu/AEAPTS/ITO surface.

In figure 2(b), peaks at 553 cm^{-1} and 823 cm^{-1} correspond to C-O and N-H bending vibrations in amino acids, respectively. Peaks seen at 3372 cm^{-1} and 1386 cm^{-1} correspond to N-H stretch and C-N stretch, respectively. Further, the peak at 1261 cm^{-1} corresponds to P-O stretch of the phosphate backbone of DNA, peaks at 1546 cm^{-1} and 1649 cm^{-1} pertain to the C-O stretch of the purine and pyrimidine rings of DNA[32]. All these peaks reveal the immobilization of the amine-terminated aptamer probe onto the silanized ITO electrode.

3.3. Electrochemical characterization

Figure 3a shows the cyclic voltammograms obtained for the ITO electrode, silane-ITO electrode, glu-silane-ITO electrode and apt-glu-silane-ITO bioelectrode in the potential range of -0.7V to +0.7V at scan rate of 50 mV/s. The 0.4V peak corresponds to the oxidation peak of the redox couple, K$_3$/K$_4$ [Fe(CN)$_6$] present in the buffer. It can be seen that there is a significant increase in the anodic peak current for the silane-ITO electrode (figure 3a (ii)) compared to that of the ITO electrode (figure 3a (i)). The NH$_2$-terminal of the silane acquires positive charge in the buffer and thus attracts the negatively charged cyanide ions present in the buffer. The electrostatic attraction between the positively charged silanized ITO surface and the negatively charged redox species present in the buffer facilitates electron transfer across the electrode-electrolyte interface leading to increased oxidation current[33]. Futher, decrease in oxidation current may perhaps be attributed to the formation of an insulating layer of glutaraldehyde on the silanized ITO surface (figure 3a (iii)). Again, the increase in the oxidation current on immobilization of the amine-terminated aptamer probe (figure 3a (iv)) can perhaps be asisgned to the electrostatic attraction between the positively charged surface of apt-glu-silane-ITO bioelectrode and the negatively charged redox species present in the buffer resulting in facile transfer of electrons.

Figure 3b shows the differential pulse voltammograms obtained for the ITO electrode, silane-ITO electrode, glu-silane-ITO electrode and apt-glu-silane-ITO bioelectrode in the potential range of -0.7V to +0.7V. The increase in the peak current for silane-ITO electrode (figure 3b (ii)) compared to that of the ITO electrode (figure 3b (i)) is attributed to the facile electron transfer aided by the opposite charges on electrode and the electrolyte. The decrease in the peak current for glu-silane-ITO electrode (figure 3b (iii)) reveals the formation of an insulating layer of glutaraldehyde. Further, increase in the current on immobilization of the amine-terminated aptamer sequence (figure 3b (iv)) is ascribed to the

transfer of electrons facilitated due to the electrostatic attraction between positive electrode surface and negative redox species in the buffer.
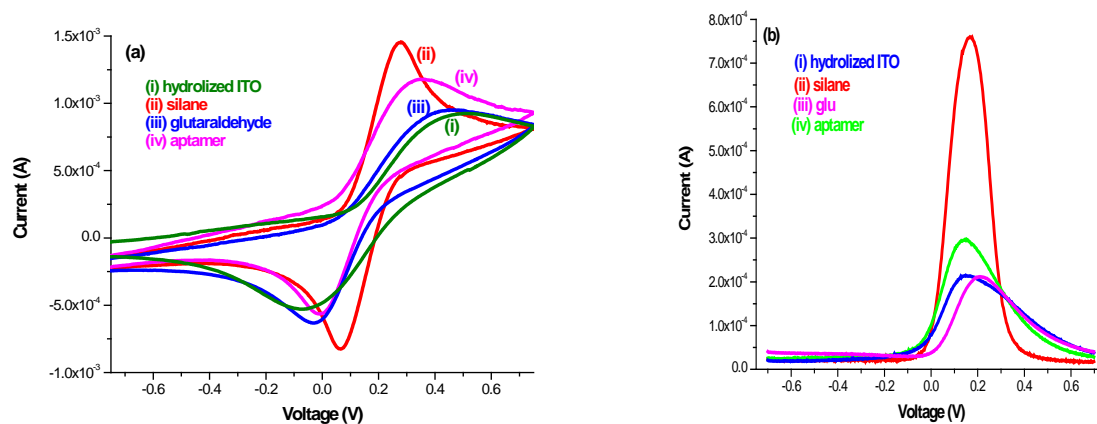

Figure 3. Stepwise characterization of aptamer functionalized bioelectrode using CV (a) and DPV (b).

3.4. Surface coverage of aptamer

The cyclic voltammteric investigations of apt-glu-silane-ITO bioelectrode have been conducted as a function of scan rate (ν) (10–100 mV/s) to determine the surface coverage of aptamer probe. The anodic peak potential (E_{pa}) is found to vary linearly with logarithm of scan rate and follows Eq.1:

$$E_{pa} = 0.2051 \log \nu - 0.0433; \quad R = 0.9949; \quad SD = 0.0046 \qquad \text{Eq.1}$$

According to Laviron's theory, the slope of the linear curve between the anodic peak potential and the logarithm of scan rate represents $RT/\alpha nF$ (α- transfer coefficient). This can be used to calculate the surface concentration of the aptamer using the following equation:

$$i_p = n^2 F^2 \nu CA (4RT)^{-1} \qquad \text{Eq.2}$$

where, i_p/ν can be calculated from the i_p Vs. ν plot (i_p- anodic peak current; ν- scan rate)[34].
The total surface concentration of the aptamer probe has been found to be 1.627×10^{-10} mol cm^{-2} (using $i_p/\nu = 9.754 \times 10^{-6}$).

3.5. Response studies of aptamer functionalized bioelectrode

The response of the aptamer functionalized bioelectrode towards target cell (A549) binding has been investigated using cyclic voltammetry in PBS buffer containing $K_3/K_4[Fe(CN)_6]$ as a redox couple in the voltage range of -0.7 V to +0.7 V at scan rate of 50 mV/s. The decrease in the oxidation current is observed due to binding of the A549 cells (figure 4a). This is because the biological cells on attachment to the substrate form an insulating layer that perhaps provides barrier to the flow of electrons through the electrode surface resulting in the decrease of the current[26]. The resistance to the flow of electrons increases with increasing concentration of A549 cells and thereby results in the decrease of current with rising concentration of target cells.

The calibration curve for the apt-glu-silane-ITO bioelectrode can be obtained by plotting the anodic peak current for logarithmic values of the different concentrations of cholesterol (figure 5(a)). Linear relation is obtained between the anodic peak current and logarithmic value of cell concentration over the range of 10^3-10^7 cells/ml with standard deviation and correlation coefficient of 62.91 µA and 0.9831, respectively.

The binding of target cells to the apt-glu-silane-ITO bioelectrode has been studied using differential pulse voltammetry. The decrease in current is observed with the increasing concentrations of target cells (figure 4b) due to formation of the insulating layer which impedes the flow of electrons through the electrode surface indicating binding of the cells to the aptamer. The calibration curve

obtained by plotting the DPV peak current for the logarithmic values of cholesterol concentrations (figure 5(b)) reveals the linearity over the concentration range of 10^3-10^7 cells/ml with standard deviation and correlation coefficient of 13.38 µA and 0.9863, respectively.
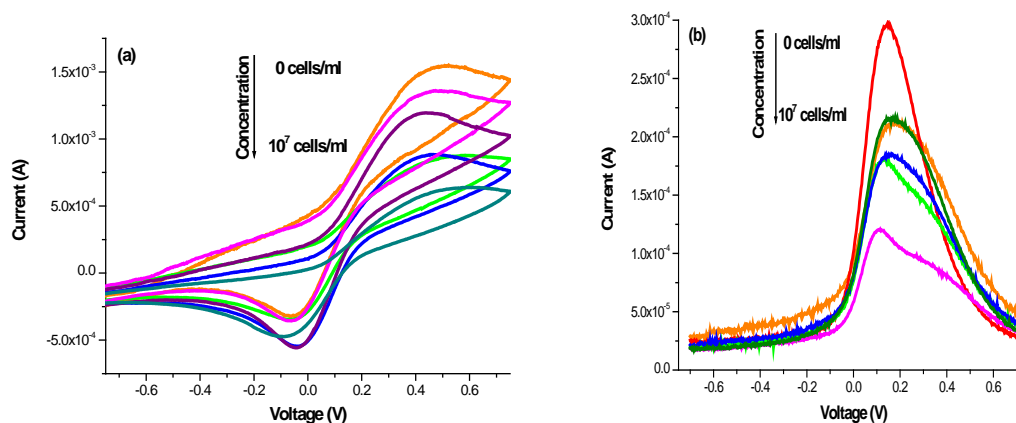

Figure 4. Response Studies of the aptamer functionalized bioelectrode using CV (a) and DPV (b) with target A549 cell concentrations of (i) 0; (ii) 10^3; (iii) 10^4 ; (iv) 10^5 ; (v) 10^6 and; (vi) 10^7 cells/ml.
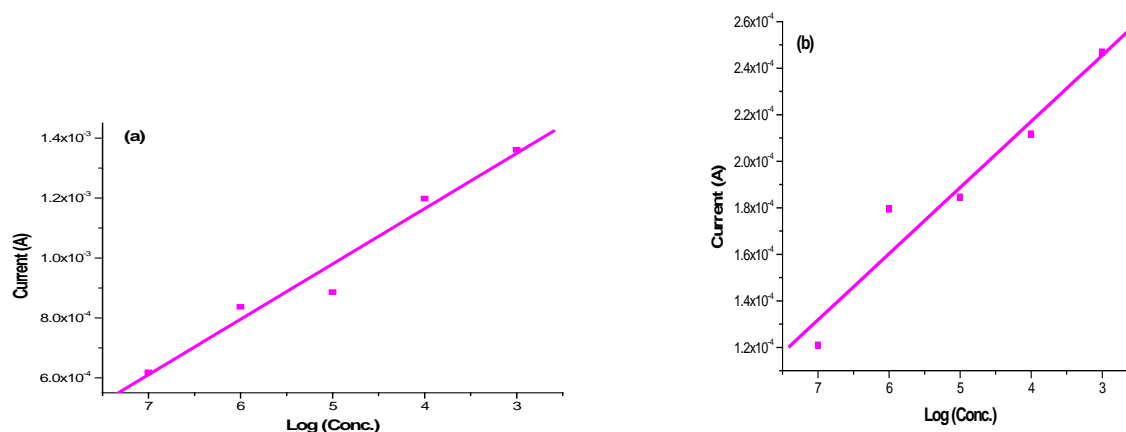

Figure 5. Calibration plot for CV response (a) and DPV response (b) of the aptamer functionalized bioelectrode towards different concentrations of A549 cells.

3.6. Response studies of aptamer functionalized bioelectrode

The specificity of the apt-glu-silane-ITO bioelectrode towards detection of A549 cells has been investigated using cyclic voltammetry (figure 6a). In the control experiments, the response of the bioelectrode towards culture medium and the control KB cells has been studied. The observed decrease in the current observed on incubation of the bioelectrode with culture medium without cells may be attributed to the physical adsorption of the species from the environment. The decrease in the current on incubation of the bioelectrode with KB cells is approximately half of that in case of A549 cells for the same concentration. Thus, the binding of the A549 cells to the bioelectrode surface perhaps dominates the CV response.

The selective response of the apt-glu-silane-ITO bioelectrode towards the A549 cells has been further confirmed by differential pulse voltammetry (figure 6b). The decrease in signal observed with the target A549 cells is much higher as compared to that obtained with culture medium and the control

KB cells. This further reveals the selectivity of the aptamer functionalized bioelectrode towards human lung adenocarcinoma A549 cells.
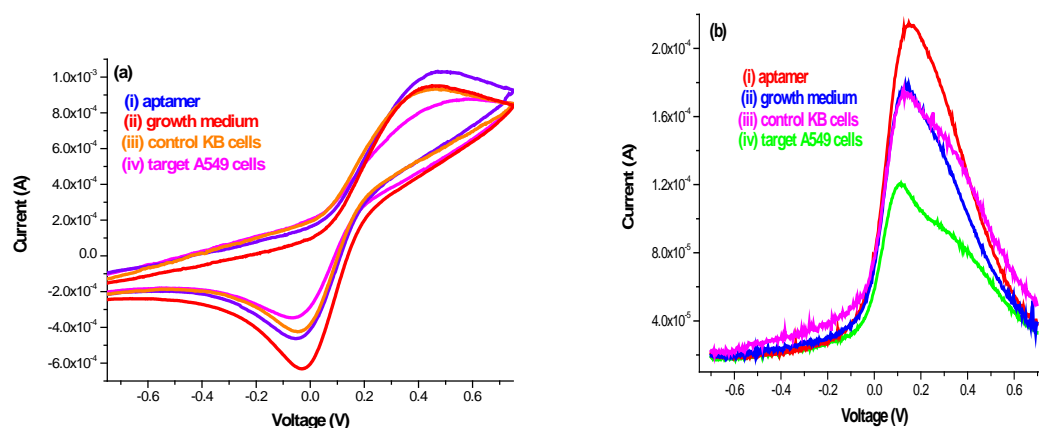

Figure 6. Specificity studies of the aptamer functionalized bioelectrode with control KB cells using CV (a) and DPV (b).

4. Conclusions

An aptamer based biosensor has been fabricated for detection of human lung adenocarcinoma A549 cells using aminosilane as the platform. The amine-terminated aptamer probe has been covalently bonded to the amine functionalized silane surface onto ITO using glutaraldehyde as the crosslinker. The surface coverage of the aptamer probe onto the silanized ITO electrode is found to be 1.627×10^{-10} mol cm^{-2}. This electrochemical aptamer sensor exhibits detection limit of 10^3 cells/ml with response time of 60 s for the target A549 cells. Aptamers show selectivity towards their target cells as the electrochemical signal response for control KB cells is about 50% as compared to that of the target cells. Thus aptamers can be utilized for the detection of the lung cancer cells. It should be interesting to utilize conducting polymers and nanomaterials including nanostructured metal oxides etc [35,36] to obtain increased sensitivity of this aptasensor.

References

[1] Kumar M, Agarwal S K and Goel S K 2009 *Mol. Cell Biochem.* **322** 73
[2] Pathak A K, Bhutani M, Mohan A, Guleria R, Bal S and Kochupillai V 2004 *Indian J. Chest Dis. Allied Sci.* **46** 191
[3] Behera D and Balamugesh T 2004 *Indian J. Chest Dis. Allied Sci.* **46** 269
[4] Sutedja G 2003 *Eur. Respir. J.* **21** 57s
[5] Mao L, Hruban R H, Boyle J O, Tockman M and Sidransky D 1994 *Cancer Res* **54** 1634
[6] Weder W, MD, Schmid R A, Bruchhaus H, Hillinger S, Schulthess G K and Steinert H C 1998 *Ann. Thorac Surg.* **66** 886
[7] Schmiemann V, Bocking A, Kazimirek M, Onofre A S C, Gabbert H E, Kappes R, Gerharz C D and Grote H J 2005 *Clin Cancer Res* **11** 7728
[8] Zhu H, Smith C, Ansah C and Gooderham N J 2005 *Cancer Cell International* **5** 28
[9] Mitsudomi T, Steinberg S M, Oie H K, Mulshine J L, Phelps R, Viallet J, Pass H, Minna J D and Gazdar A F 1991 *Cancer Res.* **51** 4999
[10] Wu W, Fan Y H, Kemp B L, Walsh G and Mao L 1998 *Cancer Res.* **58** 4082
[11] Lynch T J, Bell D W, Sordella R, Gurubhagavatula S, Okimoto R A, Haluska F G, Louis D N, Christiani D C, Settleman J and Haber D A 2004 *N. Engl. J. Med.* **350** 21
[12] Croce C M 2008 *N. Engl. J. Med.* **358** 502
[13] Li Y, Lee H J and Corn R M 2007 *Anal. Chem.* **79** 1082

[14] Li Z, Wang Y, Wang J, Tang Z, Pounds J G and Lin Y 2010 *Anal. Chem.* **82** 7008
[15] Wang H, Cao C, Li B, Chen S, Yin J, Shi J, Ye D, Tao Q, Hu P, Epstein A and Ju D 2008
      Cancer Immunol Immunother 57 677
[16] Lee T Y and Song J T 2010 *Thin Solid Films* **518** 6630
[17] Syed M A and Pervaiz S 2010 *Oligonucleotides* **20** 215
[18] Cho E J, Lee J W and Ellington A D 2009 *Annu. Rev. Anal. Chem.* **2** 241
[19] Guo K T, Paul A, Schichor C, Ziemer G and Wendel H P 2008 *Int. J. Mol. Sci.* **9** 668
[20] Mok Wand Li Y 2008 *Sensors* **8** 7050
[21] Proske D, Blank M, Buhmann R and Resch A 2005 *Appl. Microbiol. Biotechnol.* **69** 367
[22] Ishii Y, Tajima S and Kawarada H 2011 *App. Phys. Exp.* **4** 027001
[23] Prabhakar N, Matharu Z, Malhotra B D 2011 *Biosensors and Bioelectronics* **26** 4006
[24] Liu G, Mao X, Phillips J A, Xu H, Tan W and Zeng L 2009 *Anal. Chem*. **81** 10013
[25] Jie G, Wang L, Yuan J and Zhang S 2011 *Anal. Chem.* **83** 3873
[26] Pan C, Guo M, Nie Z, Xiao X, Yao S 2009 *Electroanalysis* **21** 1321
[27] Pan Y, Guo M, Nie Z, Huang Y, Pan C, Zeng K, Zhang Y and Yao S 2010 *Biosensors and*
      Bioelectronics **25** 1609
[28] Willner I and Zayats M 2007 *Angew. Chem. Int. Ed.* **46** 6408
[29] Rodriguez M C, Kawde A N and Wang J 2005 *Chem. Commun.* 4267
[30] Zhao Z, Xu L, Shi X, Tan W, Fang X and Shangguan D 2009 *Analyst* **134** 1808
[31] Das M, Sumana G, Pandey M K, Nagarajan R and Malhotra B D 2011 *Sensor Letters* **9** 499
[32] Das M, Dhand C, Sumana G, Srivastava A K, Nagarajan R, Nain L, Iwamoto M, Manaka T and
      Malhotra B D 2011 *Biomacromolecules* **12** 540
[33] Arya S K, Prusty A K, Singh S P, Solanki P R, Pandey M K, Datta M, Malhotra B D 2007 *Anal.*
      Biochem. doi:10.1016/ j.ab.2007.01.029
[34] Singh R, Dhand C, Sumana G, Verma R, Sood S, Gupta R K and Malhotra B D 2010 *J. Mol.*
      Recognit. DOI:10.1002/jmr.1014
[35] Huang Y F, Lin Y W and Lin Z H 2009 *Nanopart. Res.* **11** 775
[36] Lin M M, Kim D K, Haj A J and Dobson J 2008 *IEEE Trans. Nanobiosci.* **7** 298